Published in final edited form as:

Mol Cancer Res. 2021 October ; 19(10): 1751–1762. doi:10.1158/1541-7786.MCR-21-0239.

Mice deficient in the RNA binding protein Zfp871 are prone to early death and steatohepatitis in part through the p53-Mdm2 axis

Shakur Mohibi[1], **Jin Zhang**[1], **Mingyi Chen**[2], **Xinbin Chen**[1,*]

[1]Comparative Oncology Laboratory, Schools of Veterinary Medicine and Medicine, University of California at Davis

[2]Department of Pathology, University of Texas Southwestern Medical Center, Dallas, TX, 75390, USA

Abstract

p53 transcription factor is activated upon exposure to various cellular stresses, leading to growth suppression. However, aberrant activation of p53 can lead to defects in embryonic development and other abnormalities. Here, we identified zinc finger protein Zfp871 as a p53 target gene. We showed that as an RNA-binding protein, Zfp871 binds to Mdm2 3'UTR and stabilizes Mdm2 mRNA, which in turn suppresses p53 expression through increased expression of Mdm2 E3 ubiquitin ligase. Consistently, Zfp871 deficiency increases p53 expression, leading to growth suppression in a p53-dependent manner. To determine the role of Zfp871 in the p53 pathway, we utilized *Zfp871*-deficient mouse model and found that *Zfp871*-null mice were prone to embryonic/pre-weaning lethality, which can be partially rescued by simultaneous deletion of *Trp53*. We also found that mice heterozygous for *Zfp871* had a short lifespan and were susceptible to steatohepatitis but not to spontaneous tumors. To determine the underlying mechanism, RNA-seq analysis was performed and showed that an array of genes involved in development, lipid metabolism and inflammation are regulated by Zfp871 in conjunction with p53. Taken together, we conclude that the Zfp871-Mdm2-p53 pathway plays a critical role in tumor-free survival and development.

Keywords

Zfp871; p53; Mdm2; mRNA stability; steatohepatitis

Introduction

Tumor suppressor p53 is a potent transcription factor and can be activated upon exposure to numerous cellular stresses. p53 manifests its tumor suppressor effects by inducing senescence, cell-cycle arrest and/or apoptosis (1,2). Due to its cogent transcriptional

*Correspondence to: Xinbin Chen, xbchen@ucdavis.edu, University of California, Davis, Comparative Oncology Laboratory, 2128 Tupper Hall, VM: Surgical and Radiological Sciences, Davis, CA, 95616, (530-754-8404).

Conflict of interest: The authors have declared that no conflict of interest exists.

activity towards pro-apoptotic and cell-cycle arrest pathways, several layers for negative regulation of p53 exist that are required to maintain a fine equilibrium of p53 levels (3). This equilibrium is vital for tumor suppression, embryonic development as well as for maintaining tissue homeostasis (4). Abnormal activation of p53 during embryonic development has been linked to lethality as well as several other abnormalities that manifest through increased cell-cycle arrest and apoptosis (5,6). Even after years of extensive research on p53, most of the pathways regulating the p53 network are yet to be elucidated (1,2).

Zinc finger proteins are one of the most abundant and diverse groups of proteins with a wide range of cellular functions (7). They exhibit their key functions by binding to DNA, RNA and proteins, thereby regulating transcription, mRNA stability and protein ubiquitination, respectively (8,9). There are several families of proteins containing zinc fingers, of which the C2H2 zinc finger family is the most abundant and primarily consists of proteins with multiple repeats of zinc fingers fused with a functional domain such as the KRAB domain (8,10–12). Despite their abundance, the physiological functions for a majority of KRAB-containing zinc finger proteins remain to be characterized. Interestingly, several regulators of p53, such as Mdm2, Pirh2, and Apak (ZNF420), contain zinc fingers (13–15).

Previously, we showed that Zfp871, a KRAB-containing C2H2 zinc finger protein, interacts with Mdm2 and regulates p53 expression (16). Here, we established Zfp871 as a p53 target gene that in turn negatively regulates p53 via increased mRNA stability of Mdm2, a p53 E3 ubiquitin ligase (17). We showed the significance of the Zfp871-Mdm2-p53 pathway in growth suppression and regulation of an array of genes involved in development, lipid metabolism and inflammation. We also showed that simultaneous deletion of *Trp53* in *Zfp871*-null mice could partially rescue the embryonic/pre-weaning lethality. Notably, mice heterozygous for *Zfp871* had a shorter lifespan and were susceptible to steatohepatitis but not to spontaneous tumors. Our findings suggest that Zfp871 is an important regulator of p53 in development and disease.

Materials and Methods

Cell culture, cell line generation and reagents

SCp2 mouse mammary epithelial cells were a generous gift from Pierre-Yves Desprez (California Pacific Medical Center Research Institute) and were maintained as previously described (18). The mouse myoblast cell line C2C12, the mouse normal liver FL83B cells, human cancer cell lines HCT116, MCF-7 and RKO were obtained from ATCC between 2007 and 2018 and used below passage 20 or within 2 months of thawing. As ATCC authenticated and tested these cell lines, no further authentication and Mycoplasma testing were performed, especially considering that these cell lines were used at low passages. Mouse C2C12, mouse FL83B cells, human HCT116, MCF-7 and RKO cells were cultured in Dulbecco's modified Eagle's medium (DMEM) (Invitrogen) supplemented with 10% fetal bovine serum (FBS) (Hyclone, Logan, UT). Generation of *Zfp871-KO* C2C12 and SCp2 and *Trp53-KO* SCp2 cell lines was achieved by pSpCas9(BB)-2A-Puro vector expressing guide RNAs (Zfp871–1: 5′- GCA AAA TTT GCA GTA TAA GG −3′; Zfp871–2: 5′- TTT CAA ACT CAA CTA CCC TC −3′; p53: 5'- GAA GTC ACA GCA CAT GAC

GG - 3'). The cells were selected with puromycin, and individual clones picked, genotyped, sequenced, and confirmed by western blot analysis. The primers used for genotyping were: (1) For Zfp871, forward primer, 5'- CCC TTT AAT CGG TGA AAG AAA GCA −3', and reverse primer, 5'- GGC ACA ATG ATG CTC ACG TTA T −3'; (2) For mouse p53, forward primer, 5'- CAG CTG GCG AAG ACG TGC −3', and reverse primer, 5'- CGG GAT ACA AAT TTC CTT CCA CC −3'.

Western blot analysis

Western blotting was performed as previously described (19). Briefly, cell lysates were collected as indicated, resolved on 8–11% SDS-polyacrylamide gels and transferred to nitrocellulose membrane. After the transfer, the membranes were blocked with PBST containing 2.5% milk at room temperature (RT) for 1 hour, followed by overnight 4°C incubation with primary antibodies prepared in 2.5% milk containing PBST. The following day, after 3X washings with PBST, the blots were incubated at RT for 1 hour in secondary antibody prepared in PBST containing 2.5% milk. After 3X washings with PBST, the blots were soaked in enhanced chemiluminescence reagents (ThermoFisher Scientific™), and then visualized with the BioSpectrum 810 Imaging System (UVP LLC, Upland, CA). Antibodies used were: Mdm2 (sc-965), p21 (sc-53870), actin (sc-133155), GFP (sc-9996), PML (sc-5621), and p130 (sc-374521) purchased from Santa Cruz Biotechnology (Santa Cruz, CA); HA (W15093A) from BioLegend (San Diego, CA); p53 (#1C12) from Cell Signaling (Beverly, MA); Mdm2 (OP115) from Millipore-Sigma (Burlington, MA). Zfp871 antibody was custom-made in rabbit using amino acids 41–189 of mouse Zfp871 by Cocalico biologicals, Inc.

RNA isolation and RT-PCR

Total RNA was harvested using TRIzol reagent (Invitrogen) and isolated according to the manufacturer's instructions. RevertAid First Strand cDNA Synthesis kit (ThermoFisher Scientific™) was used to synthesize cDNA from 2 μg total RNA as per manufacturer's protocol. The primers used to amplify mouse actin were forward primer, 5'-TCC ATC ATG AAG TGT GAC GT-3', and reverse primer, 5'-TGA TCC ACA TCT GCT GGA AG-3'. The primers used to amplify Zfp871 were the same as previously described (16). The primers used to amplify mouse p21 were forward primer, 5'- GTA CTT CCT CTG CCC TGC TG −3', and reverse primer, 5'- TCT GCG CTT GGA GTG ATA GA −3'. The primers used to amplify mouse Mdm2 were forward primer, 5'- ATG AGG TCT ATC GGG TCA CAG T −3', and reverse primer, 5'- CAC ATC CAA GCC TTC TTC TGC −3'. The primers for mouse Mdm2 pre-mRNA were forward primer, 5′- CCT CAT GTT CTT TGC CTA TTT ATG −3′, and reverse primer, 5′- AGC CAG TTC TCA CGA AGG GT −3. The following program was used for PCR amplification: (i) 95 °C for 3 min, (ii) 95 °C for 30 s, (iii) 60 °C for 30 s, (iv) 72 °C for 45 s and (v) 72 °C for 5 min. From steps 2–4, the cycle was repeated 23 times for Actin and Gapdh, 25 times for p21 and Mdm2, or 26 times for Zfp871.

sgRNAs to generate knockout cell lines and siRNAs for knockdown

To generate *Zfp871-KO* cells, two single-guide RNA (sgRNA) expression vectors pSpCas9(BB)-2A-Puro-sgZfp871–1 and pSpCas9(BB)-2A-Puro-sgZfp871–2 were used to remove exon 3 and create frame shift deletions. The generation of sgRNA expression vector

was performed as described previously (20). The oligonucleotides for sgZfp871–1 are sense, 5'- CAC CGG CAA AAT TTG CAG TAT AAG G −3', and antisense, 5'- AAA CCC TTA TAC TGC AAA TTT TGC C −3'; for sgZfp871–2 are sense, 5'- CAC CGT TTC AAA CTC AAC TAC CCT C −3', and antisense, 5'- AAA CGA GGG TAG TTG AGT TTG AAA C −3'. To generate *Trp53-KO* cells, one sgRNA expression vector pSpCas9(BB)-2A-Puro-sgp53Ex5 was used to target coding region in exon 5 to create frame shift deletions. The oligonucleotides for sgp53Ex5 are sense, 5'- CAC CGG AAG TCA CAG CAC ATG ACG G −3', and antisense, 5'- AAA CCC GTC ATG TGC TGT GAC TTC C −3'.

All small interfering RNAs (siRNAs) were purchased from Dharmacon RNA Technologies (Chicago, IL). Zfp871 specific siRNAs have been described previously (16). The scrambled siRNA, 5'-GCA GUG UCU CCA CGU ACU A dTdT-3', was used as a control.

RNA-IP assay

RNA immunoprecipitation was carried out as described previously (21). Briefly, SCp2 cells and MEFs (WT and *Zfp871*$^{-/-}$) were grown to 80–90% confluence in a 100 mm dish (~2 × 10^6 cells) and cell extracts were prepared in immunoprecipitation buffer (10mM HEPES, pH 7.0, 100mM KCl, 5mM MgCl2, 0.5% Nonidet P-40, and 1mM DTT), pre-cleared with protein A/G beads, and then incubated with 2 μg of anti-Zfp871 or an isotype control IgG overnight at 4 °C. The RNA–protein immunocomplexes were brought down using magnetic protein A/G beads (MedChemExpress). Following washing and RNA-purification, RT-PCR analysis was carried out to determine the levels of Mdm2 and Gapdh transcripts.

mRNA half-life assay

To measure the mouse *Mdm2* mRNA stability, wild type and *Zfp871*$^{-/-}$ MEF cells were treated for various times with 5, 6-dichloro-1-beta-Dribofuranosylbenzimidazole (DRB), an inhibitor of transcription. The relative level of *Mdm2* mRNA was quantified using ImageJ software and normalized using the level of Actin mRNA. Values were plotted versus time and the half-life of *Mdm2* mRNA was calculated.

Mice

The use of animals and the study protocols were approved by the University of California at Davis Institutional Animal Care and Use Committee. *Zfp871*$^{+/-}$ mice were generated by the Mouse Biology Program at the University of California, Davis (Davis, CA, USA). *Trp53*$^{+/-}$ mice were obtained from the Jackson Laboratory (Sacramento, CA, USA) as described previously (22). *Zfp871*$^{+/-}$*; p53*$^{+/-}$ mice were generated by intercrossing *Zfp871*$^{+/-}$ mice with *Trp53*$^{+/-}$ mice. To genotype the *Zfp871*-WT allele, we used the forward primer, 5'-TAG TCT GGC CTC GAA CTC AGA ACC −3', and the reverse primer, 5'- TCT CAG AGG CTG CTG TGC AAG G −3'. To genotype the *Zfp871*-KO allele, we used the forward primer, 5'- GGG ATC TCA TGC TGG AGT TCT TCG −3' and reverse primer same as for WT allele. The primers to genotype *Trp53*-WT and KO alleles have been described previously (23).

Mouse embryonic fibroblast (MEF) isolation

MEFs were isolated from 12.5–13.5 days post-coitum (pc) mouse embryos, as described previously (22). To generate WT, *Trp53*$^{-/-}$ and *Zfp871*$^{-/-}$*; Trp53*$^{-/-}$ MEFs, *Zfp871*$^{+/-}$*; Trp53*$^{+/-}$ mice were inter-crossed. To generate WT, *Zfp871*$^{+/-}$ and *Zfp871*$^{-/-}$ MEFs, *Zfp871*$^{+/-}$ mice were interbred. The MEFs were cultured in DMEM supplemented with 10% FBS (Hyclone Laboratories, Erie, PA, USA), 55 μM β-mercaptoethanol and 1x non-essential amino acids solution (Cellgro, Manassas, VA, USA).

Histological analysis

Mouse tissues were fixed in 10% neutral buffered formalin, processed, and embedded in paraffin blocks. Tissue blocks were sectioned (6 μm) and stained with Hematoxylin and Eosin.

Statistical Analysis

Mice survival analysis was performed by Kaplan–Meier survival analysis using the log rank test. Data are presented as means ± standard error of the mean (SEM) or means ± standard deviation (SD). The *p* values for qRT-PCRs and colony formation assays was calculated using the two-tailed Student's *t*-tests, and $p < 0.05$ was considered statistically significant. For each experimental data point, n = 3. Excel (Microsoft, Redmond, WA) was used for statistical analyses.

Additional Materials and Methods

The detailed methods and information for RNA-seq, chromatin immunoprecipitation (ChIP), colony formation, proliferation assays and EGFP reporter assays are provided in Supplementary Materials and Methods.

Results

Zfp871 is induced by DNA damage in a p53-dependent manner

As Zfp871 is implicated in PCBP4-dependent p53 regulation (16), we examined whether Zfp871 is induced following cytotoxic stress. For this, mouse SCp2 mammary epithelial cells, in which endogenous p53 is wild-type (WT), were treated with either camptothecin (CPT) or doxorubicin (DOX) for 24 hours and examined for proteins and mRNAs of interest. We observed that the levels of Zfp871 protein and mRNA were increased with CPT or DOX treatment (Figure 1A, B and E). As positive controls, we showed that p53 and its target p21 were also increased (Figure 1A, B and E). To further test this, mouse C2C12 and FL83B cells, both of which carry an endogenous WT p53, were treated with DOX for various times. We observed that the levels of Zfp871 protein were increased 24-hour post-treatment, which sustained till 48 hours (Figures 1C and D). Similarly, we observed that the levels of Zfp871 mRNA were increased 12 hours after DNA damage and remained elevated 48 hours post DNA damage (Figures 1F and G).

To determine whether Zfp871 is induced by DNA damage in a p53-dependent manner, multiple *Trp53*$^{-/-}$ SCp2 cell lines were generated and used. As expected, the levels of basal and DNA-damage induced p21 protein and mRNA were much lower in two separate

Trp53-KO clones as compared to that in isogenic control cells (Figure 1H and I). Similarly, the levels of Zfp871 protein were much lower in *Trp53-KO* cells as compared to isogenic control. Moreover, the level of Zfp871 was not further induced by DNA damage in *Trp53-KO* cells as compared to isogenic control (Figure1H, I; Supplementary Figure S1A, B). Furthermore, the levels of Zfp871 mRNA and protein were increased by ectopic expression of p53 in *Trp53*$^{-/-}$ SCp2 cells (Figure 1J and K). These data suggest that Zfp871 is induced by DNA damage in a p53-dependent manner.

To determine whether Zfp871 is a target of p53, we searched for potential p53-responsive element(s) (p53-RE) in the genomic locus of the *Zfp871* gene. We found three putative REs – one in the promoter region and two in intron 1 of the Zfp871 gene (Figure 1L). To determine whether these putative p53-REs are recognized by p53, chromatin immunoprecipitation (ChIP) was performed and showed that p53-RE1 and p53-RE2 but, not p53-RE3, were recognized by p53 following DNA damage (Figure 1M). The binding of p53 to the p21 promoter was also detected and used as a positive control (Figure 1L-M). Thus, p53 directly regulates Zfp871 expression upon cellular stress.

Zfp871 negatively regulates mouse and human p53 expression

Several p53 target genes, such as Mdm2 and Rbm38, in turn regulate p53 expression forming a feedback loop (24,25). Thus, mouse Zfp871 was transiently expressed in multiple mouse and human cancer cells to corroborate our previous findings (16). We showed that the levels of p53 protein were decreased by over-expression of Zfp871 in mouse SCp2 and C2C12 cells as well as in human RKO, MCF7, and HCT116 cells (Figure 2A-E). These data suggest that the Zfp871-p53 loop is conserved across species, which is likely carried out by some close relatives of murine Zfp871 in humans. Conversely, we showed that upon knockdown of Zfp871, the level of p53 protein was markedly increased in mouse SCp2, C2C12, and FL83B cells (Figures 2F-H). To confirm this, we generated a cohort of *WT*, *Zfp871*$^{+/-}$ and *Zfp871*$^{-/-}$ MEFs. We observed that the levels of p53 protein along with its target p21 were increased in *Zfp871*$^{+/-}$ and *Zfp871*$^{-/-}$ MEFs as compared to *WT* MEFs from two separate MEF isolates (Figure 2I). These data indicate that Zfp871 negatively regulates mouse and human p53 expression.

Zfp871 binds and positively regulates Mdm2 mRNA stability

Mdm2 is a major regulator of p53 that controls p53 protein stability through its E3 ubiquitin ligase activity (17). Based on our earlier observations, we found that Zfp871 can regulate p53 protein stability as a part of the Mdm2 E3 ligase complex (16). However, it is also possible that Zpf871 may directly regulate Mdm2 expression to modulate p53 protein stability. Indeed, we found that the level of Mdm2 protein was decreased, whereas the level of p53 protein was increased, in *Zfp871*-KO SCp2 cells as compared to that in isogenic control (Figure 3A). On the contrary, overexpression of Zfp871 led to increased Mdm2 expression along with decreased expression of p53 (Figure 3B). These data suggest that Zfp871 regulates Mdm2 expression independent of p53. Next, to determine whether an increased expression of Mdm2 protein was due to increased expression of Mdm2 transcript by Zfp871, we measured Mdm2 mRNA in SCp2 cells transfected with Zfp871. We found that the level of Mdm2 mRNA was increased by ectopic expression of Zfp871 (Figure 3C).

To confirm this, the levels of Mdm2 protein and mRNA were examined in three different sets of MEFs. We observed that the levels of Mdm2 protein and mRNA were markedly decreased in *Zfp871*$^{-/-}$ MEFs as compared to their littermate control *WT* MEFs (Figure 3D-F; Supplementary Figure S2A-B). Of note, we did not observe a significant decrease of Mdm2 protein and only a slight decrease in Mdm2 mRNA in *Zfp871*$^{+/-}$ MEFs compared to *WT* MEFs (Supplementary Figure S2C, S2D and S2E), suggesting that Zfp871 may be haplo-insufficient in regulating Mdm2 expression. To corroborate that Zfp871 regulates Mdm2 independent of p53, the levels of Mdm2 protein were determined in WT, *Zfp871*$^{-/-}$, *Trp53*$^{-/-}$ and *Zfp871*$^{-/-}$; *Trp53*$^{-/-}$ MEFs. Consistent with the above observations, the level of Mdm2 protein was decreased in *Zfp871*$^{-/-}$ MEFs as compared to WT MEF (Figure 3G). As a target of p53, Mdm2 expression was decreased in *Trp53*$^{-/-}$ MEFs as compared to *WT* MEFs, as expected (Figure 3G). Notably, we observed that the level of Mdm2 protein was further decreased in *Zfp871*$^{-/-}$; *Trp53*$^{-/-}$ MEFs as compared to that in *Zfp871*$^{-/-}$ or *Trp53*$^{-/-}$ MEFs (Figure 3G). Moreover, Mdm2 expression was increased by ectopic expression of Zfp871 in *Zfp871*$^{-/-}$; *Trp53*$^{-/-}$ double knockout MEFs (Figure 3H). These data provide strong evidence that Zfp871 regulates Mdm2 independent of p53.

To determine whether the level of Mdm2 mRNA increased by Zfp871 is due to increased transcription or mRNA stability, we measured Mdm2 pre-mRNA by RT-PCR with one primer corresponding to the unspliced intron 11 and the other corresponding to exon 12. We showed that the levels of Mdm2 pre-mRNA were increased in *Zfp871*$^{-/-}$ and *Zfp871*$^{+/-}$ MEFs as compared to *WT* MEFs (Figure 3I; Supplementary Figure S2F). We hypothesized that loss of *Zfp871* leads to increased expression of p53 (Figure 3A), which in turn promotes transcription of Mdm2, resulting in an increased level of Mdm2 pre-mRNA. To test this, Mdm2 pre-mRNA was measured in *WT*, *Zfp871*$^{-/-}$, *Trp53*$^{-/-}$ and *Zfp871*$^{-/-}$; *Trp53*$^{-/-}$ MEFs. We observed that the increase in Mdm2 pre-mRNA seen in *Zfp871*$^{-/-}$ MEFs disappeared in *Zfp871*$^{-/-}$; *Trp53*$^{-/-}$ MEFs (Figure 3J), suggesting that the increased pre-mRNA observed upon *Zfp871*-KO is indeed a consequence of increased p53.

Based on above observations that Zfp871 increased Mdm2 pre-mRNA but decreased mature Mdm2 mRNA, we theorized that Zfp871 might bind Mdm2 mRNA and positively regulate its stability. To test this, RNA immunoprecipitation (RNA-IP) assay was performed and showed that Mdm2 mRNA was detected in anti-Zfp871 immunoprecipitates from SCp2 cells (Figure 4A) and *WT* MEFs but, not *Zfp871*$^{-/-}$ MEFs (Figure 4B). The binding of Zpf871 to Gapdh mRNA was measured as a negative control and found to be negligible (Figure 4A-B). Furthermore, to test whether Zfp871 regulates Mdm2 mRNA stability, the half-life of Mdm2 mRNA was measured in *WT* and *Zfp871*$^{-/-}$ MEFs treated with DRB (5,6-Dichlorobenzimidazole-β-D-ribofuranoside) for various times. DRB inhibits RNA polymerase II-mediated transcription elongation step and thus, impedes de novo mRNA synthesis (26). We showed that DRB treatment led to rapid decrease of Mdm2 transcript in *Zfp871*$^{-/-}$ MEFs as compared to that in *WT* MEFs (Figure 4C). The half-life was decreased from 3.75 hours in *WT* MEFs to 1.65 hours in *Zfp871*$^{-/-}$ MEFs (Figure 4D).

To further corroborate the regulation of Mdm2 mRNA stability by Zfp871 and to determine the Zfp871-binding region in Mdm2 3'UTR, 4 reporter constructs were generated (Figure 4E), which were then transfected into *Zfp871*$^{-/-}$; *Trp53*$^{-/-}$ MEFs together with varying

amounts of HA-Zfp871 expression vector. We found that ectopic expression of Zfp871 had little if any effect on expression of GFP reporter from the construct that contained only the GFP coding sequence (Figure 4F). Interestingly, Zfp871 was able to increase GFP expression from the construct in which the GFP ORF was either fused to the full-length mouse Mdm2 3'UTR or fragment A of Mdm2 3'UTR but, not fragment B (Figure 4G-I). These results suggest that Zfp871 binds the A-fragment of mouse Mdm2 3'UTR and stabilizes it.

Cells deficient in *Zfp871* are prone to cellular senescence and growth suppression in a p53-dependent manner

To assess the effect of the Zfp871-Mdm2-p53 axis on growth suppression, we created *Zfp871*-KO C2C12 and SCp2 mouse cell lines using CRISPR-Cas9. We showed that the levels of p53 protein were increased in *Zfp871*-KO and *Zfp871*-het cells (Figure 5A, D and Supplementary Figures S3A, S3D), consistent with the above observations that siRNA knockdown of Zfp871 led to increased expression of p53 in SCp2 and C2C12 cells (Figure 2F-G). To examine whether Zfp871 deficiency has an effect on cell proliferation, clonogenic assay was performed and showed that the ability of *Zfp871*-KO and *Zfp871*-het cells to form colonies was significantly decreased as compared to isogenic controls (Figures 5B, C, E and F; Supplementary Figures S3B, S3C, S3E and S3F).

To determine whether the effect of Zfp871 deficiency on cell growth is p53-dependent, Zfp871 was transiently knocked down in two separate *Trp53-KO* SCp2 clones as well as in an isogenic control clone (Figure 5G). These cells were then used for colony formation assays. When transfected with control siRNA, *Trp53-KO* cells were highly competent to form colonies as compared to isogenic control cells (Figure 5H, top panel). However, when Zfp871 was knocked down by siRNA, the ability of *Trp53-KO* cells to form colonies was not changed whereas the ability of isogenic control cells to form colonies was markedly inhibited (Figures 5H, bottom panel and Figure 5I). These data suggest that the decreased cell proliferation in Zfp871-deficient cells is p53-dependent.

Since increased p53 expression often leads to cellular senescence, we examined whether *Zfp871* deficiency has any effect on cellular senescence in $Zfp871^{-/-}$ MEFs. As the $Zfp871^{-/-}$ MEFs contained a LacZ cassette (Supplementary Figure S4A), senescence-associated β-gal staining would not be feasible to measure the extent of cells undergoing cellular senescence. Instead, various senescence markers, such as promyelocytic leukemia protein (PML) and p130, were measured. As shown in Figure 5J, PML and p130 were highly expressed in $Zfp871^{-/-}$ MEFs as compared to wild-type MEFs (Figure 5J). To further test this, a cohort of MEFs with various genotypes (WT, $Trp53^{-/-}$, $Zfp871^{-/-}$ and $Trp53^{-/-}$; $Zfp871^{-/-}$) was used for cell proliferation assay. *WT* and $Trp53^{-/-}$ MEFs showed similar growth rates (Figure 5K). Interestingly, the rate of cell proliferation was suppressed by knockout of *Zfp871*, which was restored by simultaneously knockout of *Trp53* (Figure 5K). Together, these findings indicate that increased p53 is indeed responsible for decreased cell proliferation observed in $Zfp871^{-/-}$ MEFs and Zfp871-KD SCp2 cells.

Zfp871$^{-/-}$ mice exhibit embryonic/pre-weaning lethality in part through accumulation of p53

To determine the biological function of Zfp871, we obtained *Zfp871* heterozygous mice, which were generated using the knock-out first approach at Mutant Mouse Regional Resource Center (MMRRC) (Supplementary Figure S4A and S4B). We found that *Zfp871*$^{+/-}$ mice developed normally and were fertile. However, out of 52 pups and 10 litters from *Zfp871-het* mouse interbreed, one *Zfp871*$^{-/-}$ mouse was born alive with less than half the size of *Zfp871*$^{+/-}$ littermate and survived for 17 days prior to weaning (Supplementary Table S1 and Figure S4C). These results suggest that Zfp871 is required for embryonic development and survival.

Deletion of the *Mdm2* gene in mice leads to embryonic lethality due to aberrant expression of p53, which can be rescued by simultaneous deletion of *Trp53* (27,28). Since *Zfp871* deletion increased p53 expression, we postulated that deletion of *Trp53* may render *Zfp871*$^{-/-}$ mice viable. Therefore, *Zfp871*$^{+/-}$*; Trp53*$^{+/-}$ mice were interbred, resulting in 7 litters and 33 pups. Three *Zfp871*$^{-/-}$*; Trp53*$^{+/-}$ pups were born alive, although four *Zfp871*$^{-/-}$*; Trp53*$^{+/-}$ and two *Zfp871*$^{-/-}$ pups were expected from the interbreeds based on Mendelian ratio (Supplementary Table S2). Additionally, *Zfp871*$^{-/-}$*; Trp53*$^{+/-}$ pups were only half the size of *Zfp871*$^{+/-}$*; Trp53*$^{+/-}$ littermate. Two died a day after birth and one survived for 24 days (Supplementary Figure S4C). These data suggest that embryonic lethality and pre-weaning death by deletion of *Zfp871* can be partially rescued by simultaneous deletion of *Trp53*.

Zfp871$^{+/-}$ mice have a short lifespan and are prone to steatohepatitis

As *Zfp871*$^{+/-}$ mice are viable, a cohort of *Zfp871*$^{+/-}$ mice were generated and monitored for their long-term survival and predisposition to tumors and other abnormalities. To minimize the number of animals used, the data for some of the *WT* mice were adapted from two previous studies (23,29). All the mice were derived from the same C57BL/6 background and maintained in the same facility. Since some *Zfp871*$^{+/-}$ and *WT* littermates were kept in the same cage, we observed that *Zfp871*$^{+/-}$ mice were smaller in size compared to age-matched *WT* littermates (Supplementary Figure 4D). Notably, Kaplan-Meier analysis showed that the median survival for *Zfp871*$^{+/-}$ mice (n=27; 89.3 weeks) was significantly shorter than that for *WT* mice (n=56; 117 weeks) (Figure 6A). Interestingly, like *WT* mice, *Zfp871*$^{+/-}$ mice were not prone to spontaneous tumors (Figure 6B, Supplementary Tables S3 and S4). The tumor spectrum in *Zfp871*$^{+/-}$ mice appeared very similar to *WT* mice with a few exceptions (Figure 6B). *Zfp871*$^{+/-}$ mice had one incidence of lung adenocarcinoma and hemangiopericytoma, a slightly elevated incidence of B-cell lymphoma (16.7% compared to 11.8% in WT), and no incidence of T-cell lymphoma (compared to the 3.9% in *WT*) (Figure 6B, Supplementary Tables S3 and S4).

As *Zfp871*$^{+/-}$ mice were not prone to spontaneous tumor but had a short lifespan, histological analysis was performed to examine the major organs for other potential abnormalities. We found that 96% (23 out of 24) of *Zfp871*$^{+/-}$ mice, whereas only 4% (2 out of 51) of WT mice, had splenic/thymic hyperplasia (Figure 6C). We also found that 42% of *Zfp871*$^{+/-}$ but none of *WT* mice were prone to inflammation in 2 or more

organs (Figure 6D). Notably, 50% (12 out of 24) of *Zfp871*$^{+/-}$ mice, whereas just 6% (3 out of 51) of *WT* mice, developed steatohepatitis (Figure 6E-F). As steatohepatitis often leads to liver cirrhosis and eventually liver failure (30), we conclude that the high incidence of steatohepatitis and chronic inflammation are likely responsible for the shorter lifespan observed in *Zfp871*$^{+/-}$ mice.

Several key developmental pathways as well as genes involved in lipid metabolism and inflammation are regulated by Zfp871 in conjunction with p53

To explain the mouse phenotypes observed upon Zfp871 deficiency, RNA-seq was performed to determine the genes and pathways regulated by Zfp871. As *Zfp871* deletion leads to increased p53 expression, we wanted to determine the pathways regulated by Zfp871 in conjunction with p53 and the ones regulated by Zfp871 independent of p53. For this, total RNAs were purified from a cohort of *WT*, *Zfp871*$^{-/-}$, *Trp53*$^{-/-}$ and *Zfp871*$^{-/-}$*; Trp53*$^{-/-}$ MEFs at passage 4 for RNA-seq. Venn diagram showed that both common and distinct groups of genes were expressed among these MEFs (Supplementary Figure S5A). Heat-map analysis revealed that several groups of genes were differentially expressed in *Zfp871*$^{-/-}$ MEFs in a p53-dependent manner (Supplementary Figure S5B). To determine the number of genes that were regulated by Zfp871 in conjunction with p53, we compared gene expression patterns between WT and *Zfp871*$^{-/-}$ MEFs (Supplementary Figure S5C). We found that Zfp871 and p53 coordinately up-regulated 643 genes and down-regulated 953 genes (Supplementary Figure S5C). Similarly, to determine genes regulated by Zfp871 independent of p53, we compared gene expression patterns between *Trp53*$^{-/-}$ and *Zfp871*$^{-/-}$*; Trp53*$^{-/-}$ MEFs (Supplementary Figure S5D). Interestingly, we observed that the number of genes regulated by Zfp871 alone (493 genes) were less than a third of the number regulated by both Zfp871 and p53 (1496 genes) (Supplementary Figure S5D). This suggests that the repertoire of pathways regulated by Zfp871 is substantially increased by p53. Next, to look at various pathways regulated by Zfp871 alone or together with p53, we performed gene set enrichment analysis (Supplementary Figures S5E and S5F). Notably, several pathways vital for cell and embryonic development were found to be regulated by Zfp871 in combination with p53 (Supplementary Figure S5E). Nevertheless, Zfp871 alone was able to regulate pathways that are important for cell migration and for cellular response to interferon-beta (Supplementary Figure S5F). Furthermore, we looked for differentially expressed genes that are involved in the development of steatohepatitis. We found that several genes involved in fatty acid metabolism and inflammation were differentially expressed in *Zfp871*$^{-/-}$ MEFs as compared to WT MEFs (Supplementary Table S5), suggesting that altered lipid metabolism and inflammation by ZFP871 deficiency is likely responsible for steatohepatitis.

Discussion

The tumor suppressor p53 plays a vital role in cell growth and survival through its transcriptional activity (1,2). Interestingly, multiple p53-induced genes come back to negatively or positively regulate p53, forming a feedback loop. In this study, we found that p53 transcriptionally regulates Zfp871, which in turn negatively regulates p53. We

also showed that *Zfp871*-KO leads to growth suppression and cellular senescence in a p53-dependent manner.

p53 is known to be a short-lived protein regulated through protein stability (31). Accordingly, several E3 ubiquitin ligases are known to target p53 for degradation, of which Mdm2 is a well-defined one (31). Previously, we showed that Zfp871 negatively regulates p53 protein stability as part of Mdm2 E3 ubiquitin ligase complex through association with Mdm2 (16). Additionally, through the KRAB domain present in its N-terminus, Zfp871 may interact with KRAB-associated protein-1 (KAP1, also called TRIM28), which in turn has been shown to regulate p53 protein stability as a part of Mdm2 E3 ubiquitin ligase complex (32). Here we found that as an RNA-binding protein, Zfp871 binds to Mdm2 3'UTR, positively regulating Mdm2 mRNA stability and consequently p53 protein stability. This is in accordance with the reported dual activities of Zfp871 to act as a transcription factor and as an RNA-binding protein (33). Interestingly, in contrast to the decrease in mature Mdm2 mRNA upon Zfp871 KO, we observed increased Mdm2 pre-mRNA. This contrast seems to be the result of increased levels of p53 protein upon depletion of Zfp871, which would then lead to increased transcription and subsequently, elevated levels of Mdm2 pre-mRNA. On the other hand, loss of Zfp871 leads to decreased stability of Mdm2 mature mRNA as most RNA-binding proteins are known to regulate the stability of processed mature mRNA and not the pre-mRNA (34). Thus, Zfp871 regulates p53 protein stability as a part of the Mdm2 complex but also as a regulator of Mdm2 expression.

KRAB-containing C2H2 zinc finger proteins form the largest family of mammalian transcription factors. However, the biological functions for most of the family proteins are not known (7). To determine the biological function of Zfp871, we employed a *Zfp871*-deficient mouse model. Interestingly, we were unable to obtain *Zfp871* knock-out mice at Mendelian ratios at birth, which we theorized could be due to increased p53 levels, leading to embryonic lethality (6,27,28). Thus, we investigated if we could obtain $Zfp871^{-/-}$ mice with simultaneous deletion of *Trp53*. While we were able to obtain $Zfp871^{-/-}; Trp53^{+/-}$ pups close to Mendelian ratio, these mice died soon after birth, indicating a partial rescue. Thus, RNA-seq was performed and showed that multiple key developmental pathways are regulated by Zfp871 in conjunction with p53, suggesting that alteration of these developmental pathways is likely responsible for the incomplete rescue observed in these mice. Nonetheless, our study indicated that p53 is a critical effector of Zfp871 function.

We found that $Zfp871^{+/-}$ mice have a short lifespan. Because $Zfp871^{+/-}$ mice are not prone to spontaneous tumors but to chronic inflammation in multiple organs, especially steatohepatitis, we postulate that steatohepatitis/NASH is likely responsible for the shortened lifespan. NASH is one of the most common forms of liver disease in the Western economies as well as a major cause of liver failure resulting in death (30). Although NASH is frequently associated with obesity and diabetes, it can be triggered by changes in gene expression (35). Accordingly, increased levels of p53 protein have been shown to correlate with increase in NASH severity in mice as well as in human patients (36–38). Additionally, loss of Zfp871 leads to altered expression of multiple genes necessary for lipid metabolism and inflammation, which would synergize with increased expression of p53 to promote steatohepatitis. It should be mentioned here that although we could not find a human zinc

finger protein with more than 50% sequence homology with Zfp871 protein, there could be functional homologs of Zfp871 in humans that regulate p53 protein stability in a similar mechanism. Taken together, we conclude that the Zfp871-Mdm2-p53 pathway plays an indispensable role in development and long-term survival.

Supplementary Material

Refer to Web version on PubMed Central for supplementary material.

Acknowledgements

We would like to thank members of the Chen-Zhang laboratory for suggestions and helpful discussions. This work is supported in part by National Institutes of Health grants [CA195828, CA224433, and CA250338 to XC].

Financial support:

NIH grants CA195828, CA250338, and CA224433

Data Availability Statement

The RNA-sequencing datasets from this publication have been submitted to the GEO database and have been assigned the following Series record: GSE176582.

References

1. Vousden KH, Prives C. Blinded by the Light: The Growing Complexity of p53. Cell2009. page 413–31.
2. Levine AJ, Oren M. The first 30 years of p53: Growing ever more complex. Nat. Rev. Cancer2009. page 749–58. [PubMed: 19776744]
3. Choi J, Donehower LA. p53 in embryonic development: Maintaining a fine balance. Cell. Mol. Life Sci1999. page 38–47. [PubMed: 10065150]
4. Grier JD, Xiong S, Elizondo-Fraire AC, Parant JM, Lozano G. Tissue-Specific Differences of p53 Inhibition by Mdm2 and Mdm4. Mol Cell Biol2006;
5. Van Nostrand JL, Brady CA, Jung H, Fuentes DR, Kozak MM, Johnson TM, et al. Inappropriate p53 activation during development induces features of CHARGE syndrome. Nature2014;514:228–32. [PubMed: 25119037]
6. Zhang M, Zhang Y, Xu E, Mohibi S, De Anda DM, Jiang Y, et al. Rbm24, a target of p53, is necessary for proper expression of p53 and heart development. Cell Death Differ2018;25. [PubMed: 30349078]
7. Cassandri M, Smirnov A, Novelli F, Pitolli C, Agostini M, Malewicz M, et al. Zinc-finger proteins in health and disease. Cell Death Discov2017.
8. Emerson RO, Thomas JH. Adaptive evolution in zinc finger transcription factors. PLoS Genet2009;5.
9. Gamsjaeger R, Liew CK, Loughlin FE, Crossley M, Mackay JP. Sticky fingers: zinc-fingers as protein-recognition motifs. Trends Biochem. Sci2007. page 63–70. [PubMed: 17210253]
10. Yang P, Wang Y, Macfarlan TS. The Role of KRAB-ZFPs in Transposable Element Repression and Mammalian Evolution. Trends Genet2017. page 871–81. [PubMed: 28935117]
11. Imbeault M, Helleboid PY, Trono D. KRAB zinc-finger proteins contribute to the evolution of gene regulatory networks. Nature2017;543:550–4. [PubMed: 28273063]
12. Najafabadi HS, Mnaimneh S, Schmitges FW, Garton M, Lam KN, Yang A, et al. C2H2 zinc finger proteins greatly expand the human regulatory lexicon. Nat Biotechnol2015;33:555–62. [PubMed: 25690854]

13. Lee JT, Gu W. The multiple levels of regulation by p53 ubiquitination. Cell Death Differ2010. page 86–92. [PubMed: 19543236]
14. Shloush J, Vlassov JE, Engson I, Duan S, Saridakis V, Dhe-paganon S, et al. Structural and functional comparison of the RING domains of two p53 E3 ligases, Mdm2 and Pirh2. J Biol Chem2011;286:4796–808. [PubMed: 21084285]
15. Tian C, Xing G, Xie P, Lu K, Nie J, Wang J, et al. KRAB-type zinc-finger protein Apak specifically regulates p53-dependent apoptosis. Nat Cell Biol2009;11:580–91. [PubMed: 19377469]
16. Yan W, Scoumanne A, Jung YS, Xu E, Zhang J, Zhang Y, et al. Mice deficient in poly(C)-binding protein 4 are susceptible to spontaneous tumors through increased expression of ZFP871 that targets p53 for degradation. Genes Dev [Internet]. Comparative Oncology Laboratory, School of Veterinary Medicine, School of Medicine, University of California at Davis, Davis, California 95616, USA.; 2016;30:522–34. Available from: https://www.ncbi.nlm.nih.gov/pubmed/26915821
17. Haupt Y, Maya R, Kazaz A, Oren M. Mdm2 promotes the rapid degradation of p53. Nature1997;387:296–9. [PubMed: 9153395]
18. Desprez PY, Hara E, Bissell MJ, Campisi J. Suppression of mammary epithelial cell differentiation by the helix-loop-helix protein Id-1. Mol Cell Biol1995;15:3398–404. [PubMed: 7760836]
19. Mohibi S, Zhang J, Chen X. PABPN1, a Target of p63, Modulates Keratinocyte Differentiation through Regulation of p63α mRNA Translation. J Invest Dermatol [Internet]. 2020;140:2166–2177.e6. Available from: https://linkinghub.elsevier.com/retrieve/pii/S0022202X20312562
20. Ran FA, Hsu PD, Wright J, Agarwala V, Scott DA, Zhang F. Genome engineering using the CRISPR-Cas9 system. Nat Protoc [Internet]. Nature Publishing Group, a division of Macmillan Publishers Limited. All Rights Reserved.; 2013;8:2281. Available from: 10.1038/nprot.2013.143
21. Peritz T, Zeng F, Kannanayakal TJ, Kilk K, Eiríksdóttir E, Langel U, et al. Immunoprecipitation of mRNA-protein complexes. Nat Protoc2006;1:577–80. [PubMed: 17406284]
22. Zhang J, Cho SJ, Shu L, Yan W, Guerrero T, Kent M, et al. Translational repression of p53 by RNPC1,a p53 target over expressed in lymphomas. Genes Dev [Internet]. 2011/07/19. Comparative Cancer Center, Schools of Medicine and Veterinary Medicine, University of California at Davis, USA.; 2011;25:1528–43. Available from: https://www.ncbi.nlm.nih.gov/pubmed/21764855
23. Zhang Y, Qian Y, Zhang J, Yan W, Jung YS, Chen M, et al. Ferredoxin reductase is critical for p53-dependent tumor suppression via iron regulatory protein 2. Genes Dev2017;31:1243–56. [PubMed: 28747430]
24. Shu L, Yan W, Chen X. RNPC1, an RNA-binding protein and a target of the p53 family, is required for maintaining the stability of the basal and stress-induced p21 transcript. Genes Dev [Internet]. 2006/10/20. Department of Cell Biology, The University of Alabama at Birmingham, Birmingham, AL 35294, USA.; 2006;20:2961–72. Available from: https://www.ncbi.nlm.nih.gov/pubmed/17050675
25. Barak Y, Juven T, Haffner R, Oren M. Mdm2 Expression Is Induced By Wild Type P53 Activity. EMBO J [Internet]. 1993;12:461–8. Available from: http://www.ncbi.nlm.nih.gov/pubmed/8440237%0Ahttp://www.pubmedcentral.nih.gov/articlerender.fcgi?artid=PMC413229
26. Zandomeni R, Carrera Zandomeni M, Shugar D, Weinmann R. Casein kinase type II is involved in the inhibition by 5,6-dichloro-1-β-D-ribofuranosylbenzimidazole of specific RNA polymerase II transcription. J Biol Chem1986;261:3414–9. [PubMed: 3456346]
27. Luna RMDO, Wagner DS, Lozano G. Rescue of early embryonic lethality in mdm2-deficient mice by deletion of p53. Nature1995;
28. Jones SN, Roe AE, Donehower LA, Bradley A. Rescue of embryonic lethality in Mdm2-deficient mice by absence of p53. Nature1995;378:206–8. [PubMed: 7477327]
29. Yang HJ, Zhang J, Yan W, Cho SJ, Lucchesi C, Chen M, et al. Ninjurin 1 has two opposing functions in tumorigenesis in a p53-dependent manner. Proc Natl Acad Sci U S A2017;114:11500–5. [PubMed: 29073078]
30. Sanches SCL, Ramalho LNZ, Augusto MJ, Da Silva DM, Ramalho FS. Nonalcoholic Steatohepatitis: A Search for Factual Animal Models. Biomed Res. Int2015.

31. Pant V, Lozano G. Limiting the power of p53 through the ubiquitin proteasome pathway. Genes Dev2014. page 1739–51. [PubMed: 25128494]
32. Wang C, Ivanov A, Chen L, Fredericks WJ, Seto E, Rauscher FJ, et al. MDM2 interaction with nuclear corepressor KAP1 contributes to p53 inactivation. EMBO J2005;24:3279–90. [PubMed: 16107876]
33. Han H, Braunschweig U, Gonatopoulos-Pournatzis T, Weatheritt RJ, Hirsch CL, Ha KCH, et al. Multilayered Control of Alternative Splicing Regulatory Networks by Transcription Factors. Mol Cell2017;65:539–553.e7. [PubMed: 28157508]
34. Mohibi S, Chen X, Zhang J. Cancer the'RBP'eutics–RNA-binding proteins as therapeutic targets for cancer. Pharmacol Ther [Internet]. 2019;203:107390. Available from: https://linkinghub.elsevier.com/retrieve/pii/S0163725819301275
35. Dongiovanni P, Anstee Q, Valenti L. Genetic Predisposition in NAFLD and NASH: Impact on Severity of Liver Disease and Response to Treatment. Curr Pharm Des2013;19:5219–38. [PubMed: 23394097]
36. Tomita K, Teratani T, Suzuki T, Oshikawa T, Yokoyama H, Shimamura K, et al. P53/p66Shc-mediated signaling contributes to the progression of non-alcoholic steatohepatitis in humans and mice. J Hepatol2012;57:837–43. [PubMed: 22641095]
37. Yahagi N, Shimano H, Matsuzaka T, Sekiya M, Najima Y, Okazaki S, et al. p53 Involvement in the pathogenesis of fatty liver disease. J Biol Chem2004;279:20571–5. [PubMed: 14985341]
38. Farrell GC, Larter CZ, Hou JY, Zhang RH, Yeh MM, Williams J, et al. Apoptosis in experimental NASH is associated with p53 activation and TRAIL receptor expression. J Gastroenterol Hepatol2009;24:443–52. [PubMed: 19226377]

Implications:

A fine equilibrium of p53 is required for preventing damaging effects of aberrant p53 expression. We identify the Zfp871-Mdm2-p53 pathway that plays a critical role in development of mice and steatohepatitis.

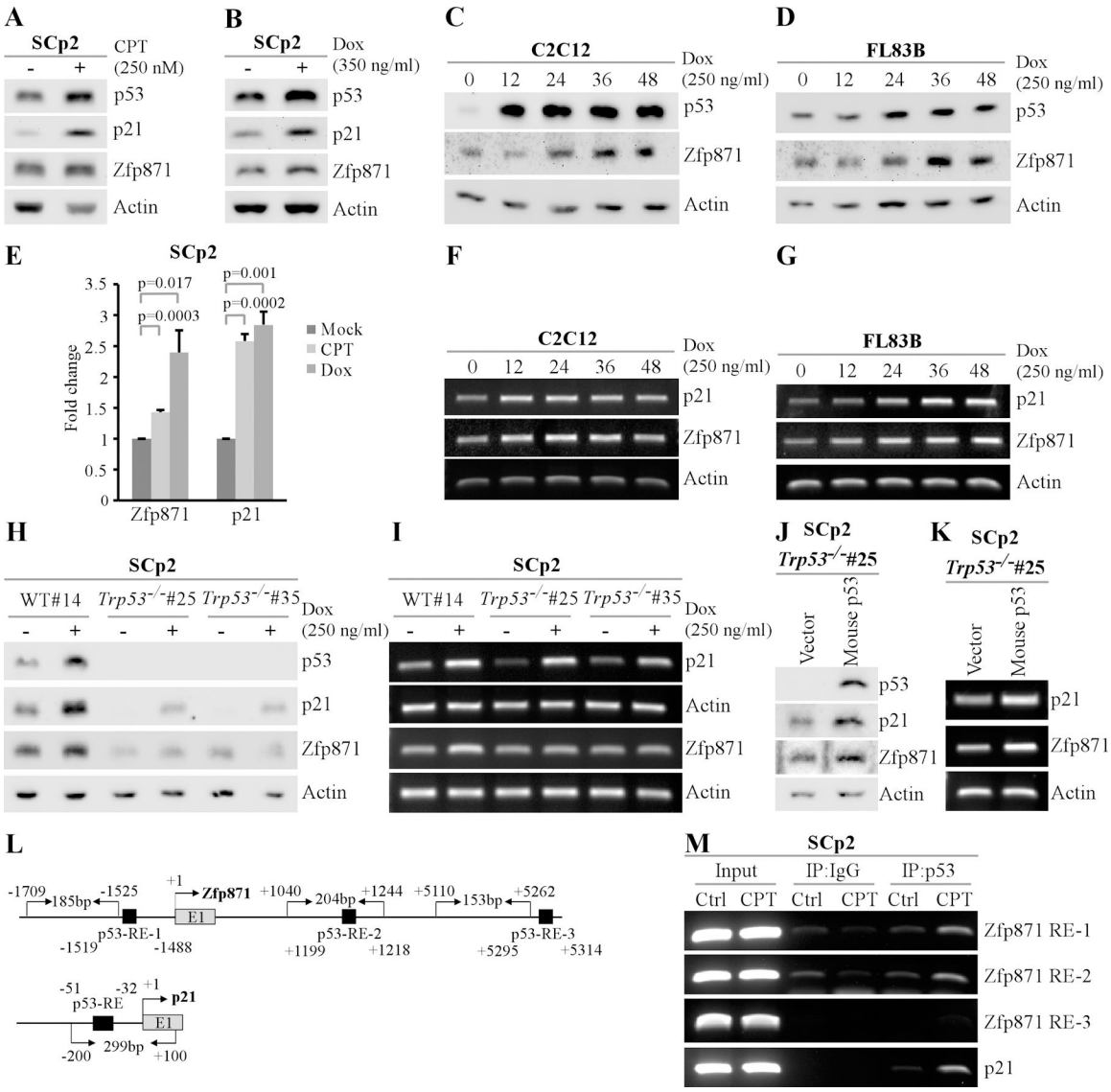

Figure 1- Zfp871 is induced by DNA damage in a p53-dependent manner.

(**A, B**) The levels of p53, p21, Zfp871 and Actin proteins were measured by western blotting in SCp2 cells mock-treated or treated with 250 nM CPT (A) or 350 μg/ml Dox (B) for 24 h. (**C, D**) The levels of p53, Zfp871 and Actin were measured in C2C12 (C) and FL83B (D) cells mock-treated or treated with 250 μg/ml Dox for 12–48 h. (**E**) The levels of Zfp871 and p21 mRNAs were measured by qRT-PCR in SCp2 cells mock-treated or treated with 250 nM CPT or 350 μg/ml Dox for 24 h. (**F, G**) The levels of p21, Zfp871 and Actin mRNA were measured by RT-PCR in C2C12 (F) and FL83B (G) cells mock-treated or treated with 250 μg/ml Dox for 12–48 h. (**H, I**) The levels of p53, p21, Zfp871, and Actin proteins (H) and mRNAs (I) were measured in isogenic control and *Trp53*$^{-/-}$ SCp2 (clone #25 or #35) cells, which were mock-treated or treated with 350 μg/ml Dox for 24 h. (**J, K**) The levels of p53, p21, Zfp871, and Actin proteins (J) and mRNAs (K) were measured in *Trp53*$^{-/-}$ SCp2 (clone #25) cells that were transiently transfected with either empty vector or mouse p53 for 24 h. (**L**) Schematic diagrams of the Zfp871 and p21 promoters along with putative p53-RE

sites. Also shown are the locations of primers on Zfp871 and p21 promoters for chromatin immunoprecipitation (ChIP) assays. (**M**) Cell lysates purified from SCp2 cells mock-treated or treated with 200 nM CPT for 16 h were immunoprecipitated with control IgG or anti-p53 antibody, followed by RT-PCR to determine the binding of p53 to the p53 REs in the Zfp871 and p21 promoters.

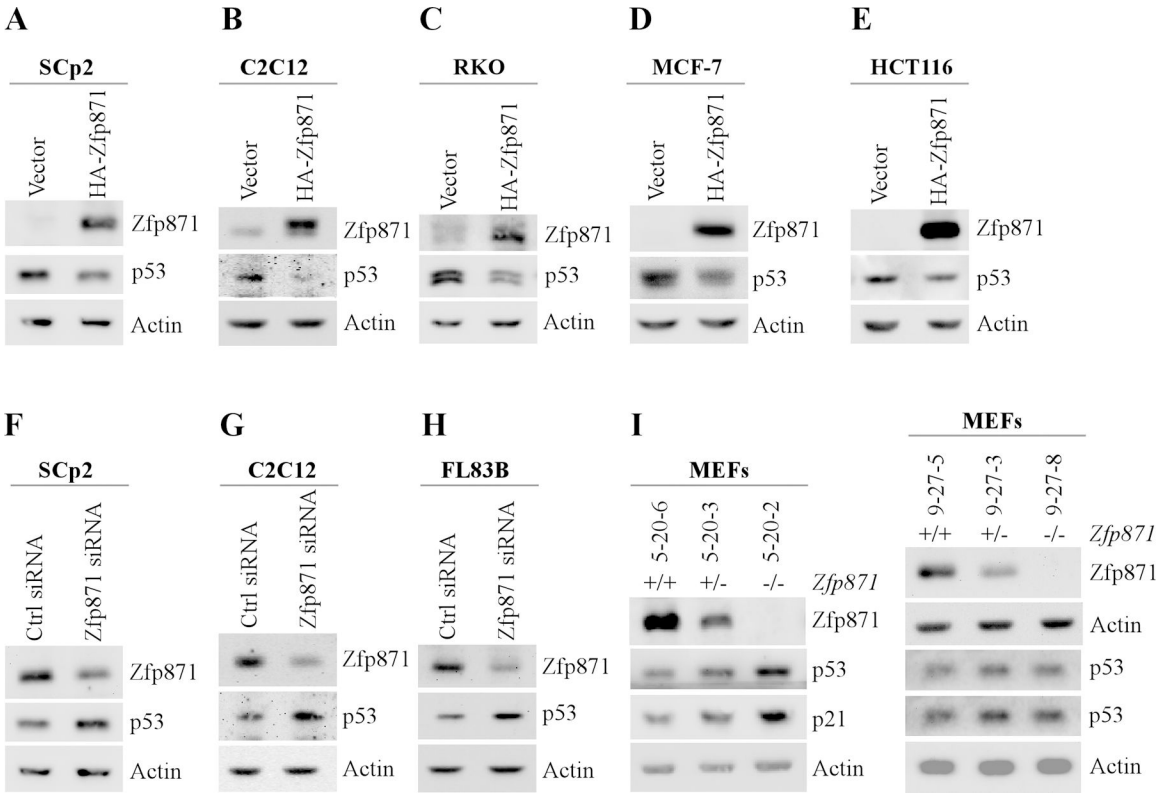

Figure 2 - Zfp871 negatively regulates mouse and human p53 expression.

(**A-E**) The levels of Zfp871, p53 and Actin proteins were measured by western blotting in SCp2 (A), C2C12 (B), RKO (C), MCF7 (D) and HCT116 (E) cells that were transiently transfected with either empty vector or HA-Zfp871 for 24 h. (**F-H**) The levels of Zfp871, p53 and Actin proteins were measured in SCp2 (F), C2C12 (G) and FL83B (H) cells that were transfected with 50 nM control or Zfp871 siRNA for 72 h. (**I**) The levels of Zfp871, p53, p21, and Actin were measured in two sets of WT, *Zfp871*$^{+/-}$, and *Zfp871*$^{-/-}$ MEFs. Low and high exposures of the same p53 blot are shown in the right panel.

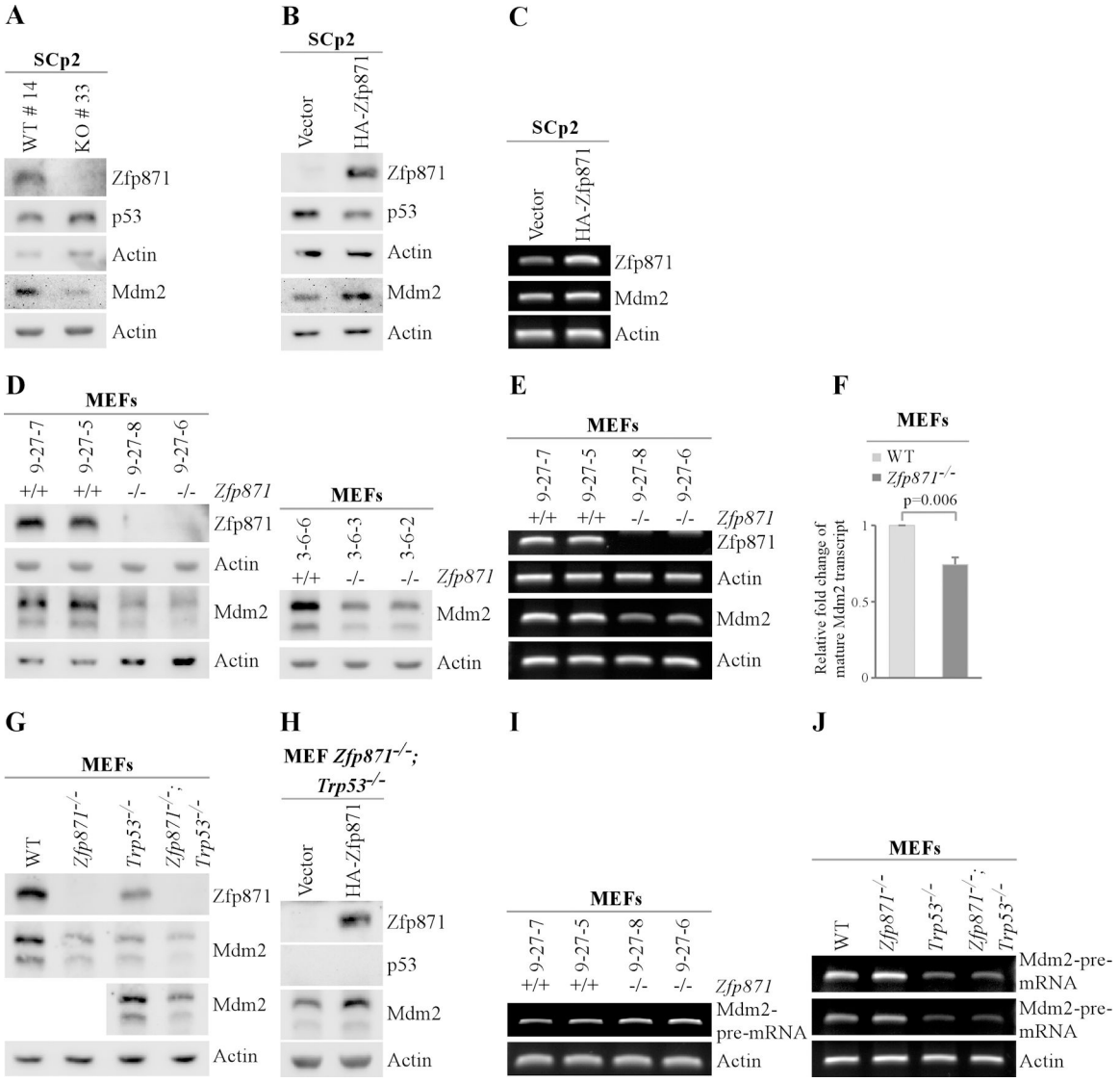

Figure 3 - Loss of Zfp871 leads to decreased expression of Mdm2 protein and transcript.

(**A**) The levels of Zfp871, p53, Mdm2 and Actin proteins were measured by western blotting in isogenic control and *Zfp871*$^{-/-}$ clone #33. (**B, C**) The levels of Zfp871, p53, Mdm2 and Actin proteins (B) and mRNAs (C) were measured in SCp2 cells transiently transfected with either empty vector or HA-Zfp871 for 24 h. The Zfp871, p53 and Actin blots depicted in Figure 3B are the same as the ones shown in Figure 2A as the same lysates were used to probe Mdm2 and Actin. (**D, E**) The levels of Zfp871, Mdm2, and Actin proteins (D) and mRNAs (E) were measured in two sets of WT and *Zfp871*$^{-/-}$ MEFs. (**F**) The levels of Mdm2 mRNA were measured by qRT-PCR in WT and *Zfp871*$^{-/-}$ MEFs. (**G**) The levels of Zfp871, Mdm2, and Actin proteins were measured in WT, *Zfp871*$^{-/-}$, *Trp53*$^{-/-}$, and *Zfp871*$^{-/-}$; *Trp53*$^{-/-}$ MEFs. Low and high exposures of the same Mdm2 blot are shown. (**H**) The levels of Zfp871, p53, Mdm2 and Actin proteins were measured in *Zfp871*$^{-/-}$; *Trp53*$^{-/-}$ MEFs transiently transfected with empty vector or HA-Zfp871 for 24 h. (**I, J**) The levels of Mdm2 pre-mRNA were measured by RT-PCR in WT, *Zfp871*$^{-/-}$, *Trp53*$^{-/-}$, and *Zfp871*$^{-/-}$;

Trp53$^{-/-}$ MEFs as indicated. Low and high exposures of the Mdm2 pre-mRNA from the same gel are shown in Figure 3J.

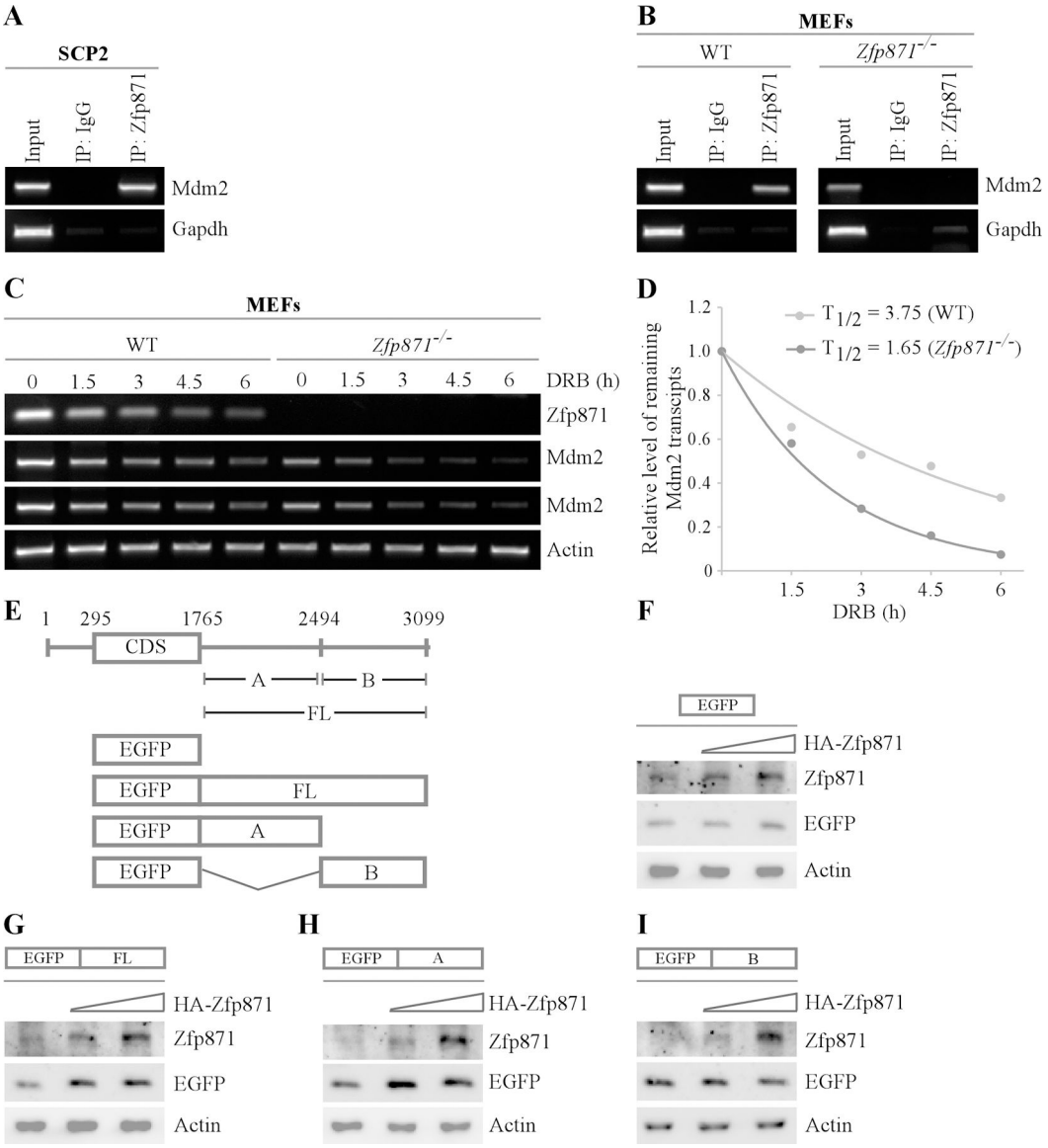

Figure 4 - Zfp871 binds to Mdm2 transcript and positively regulates Mdm2 mRNA stability.

(**A**) Lysates from SCp2 cells were subjected to RNA-IP using anti-Zfp871 antibody to determine the binding of Zfp871 to Mdm2 mRNA. The binding of Zfp871 to Gapdh mRNA was used as a negative control. Control IgG was used as a RNA-IP control. (**B**) RNA-IP experiment was performed as in (A) except lysates from WT and *Zfp871*$^{-/-}$ MEFs were used. (**C**) The levels of Zfp871, Mdm2 and Actin transcripts were measured in WT and *Zfp871*$^{-/-}$ MEFs mock-treated or treated with DRB for indicated times. Low and high exposures of the Mdm2 transcript from the same gel are shown. (**D**) The relative levels of Mdm2 transcript in (C) were normalized to actin and the half-life of Mdm2 transcript was calculated by plotting the remaining mRNA over time. (**E**) Schematic representation of the mouse Mdm2 transcript and the locations of three 3'UTR fragments in EGFP reporter vectors. (**F-I**) Various amounts of HA-Zfp871 expression vector were transfected into *Zfp871*$^{-/-}$; *Trp53*$^{-/-}$ MEFs together with a fixed amount of EGFP only (F) or EGFP plus

Full-length (FL) Mdm2 3’UTR (G), EGFP plus fragment-A (H), or EGFP plus fragment-B (I). The levels of HA-Zfp871, EGFP and actin proteins were examined by western blotting.

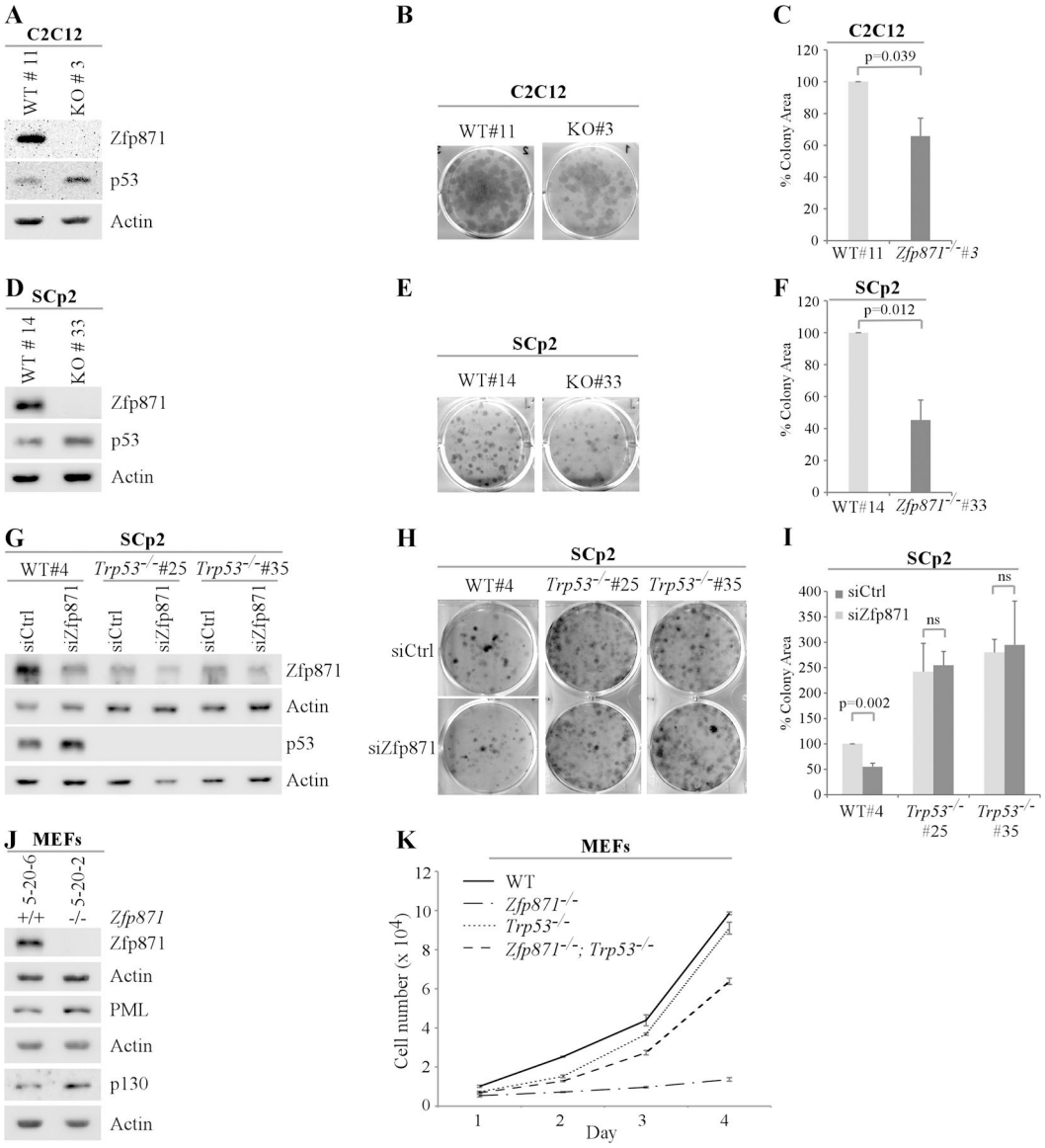

Figure 5 - Cells deficient in Zfp871 are prone to cellular senescence and growth suppression in a p53-dependent manner.

(**A, D**) The levels of Zfp871, p53 and Actin proteins were measured in isogenic control and *Zfp871*$^{-/-}$ C2C12 (clone #3) cells (A) or isogenic control and *Zfp871*$^{-/-}$ SCp2 (clone #33) cells (D). (**B, E**) Isogenic control and *Zfp871*$^{-/-}$ C2C12 (clone #3) cells (B) or isogenic control and *Zfp871*$^{-/-}$ SCp2 (clone #33) cells (E) were plated for colony formation assays and grown for one week followed by fixation with methanol: acetic acid (7:1) and staining with crystal violet. (**C, F**) The colonies obtained from the experiments in B and E were quantified using ColonyArea in ImageJ software and plotted as percentage of colony area. The density of colonies from isogenic control cells was set at 100%. (**G**) The levels of Zfp871, p53, and Actin proteins (G) were measured in isogenic control, *Trp53*$^{-/-}$ #25, and *Trp53*$^{-/-}$ #35 SCp2 cells transfected with control or Zfp871 siRNA for 72 h. (**H**) The cells treated as in (G) were plated for colony formation assays 24 h after transfection and grown for one week followed by fixing with fixation with methanol: acetic acid (7:1) and staining

with crystal violet. (**I**) The colonies obtained from the experiment in (H) were quantified using ColonyArea in ImageJ software and plotted as percentage colony area. The density of colonies from isogenic control cells transfected with control siRNA was set at 100%. (**J**) The levels of Zfp871, PML, p130, and Actin proteins were measured in WT and *Zfp871*$^{-/-}$ MEFs. (**K**) The rate of cell proliferation was measured for WT, *Zfp871*$^{-/-}$, *Trp53*$^{-/-}$, and *Zfp871*$^{-/-}$*; Trp53*$^{-/-}$ MEFs plated in a 6-well plate over a 4-day period.

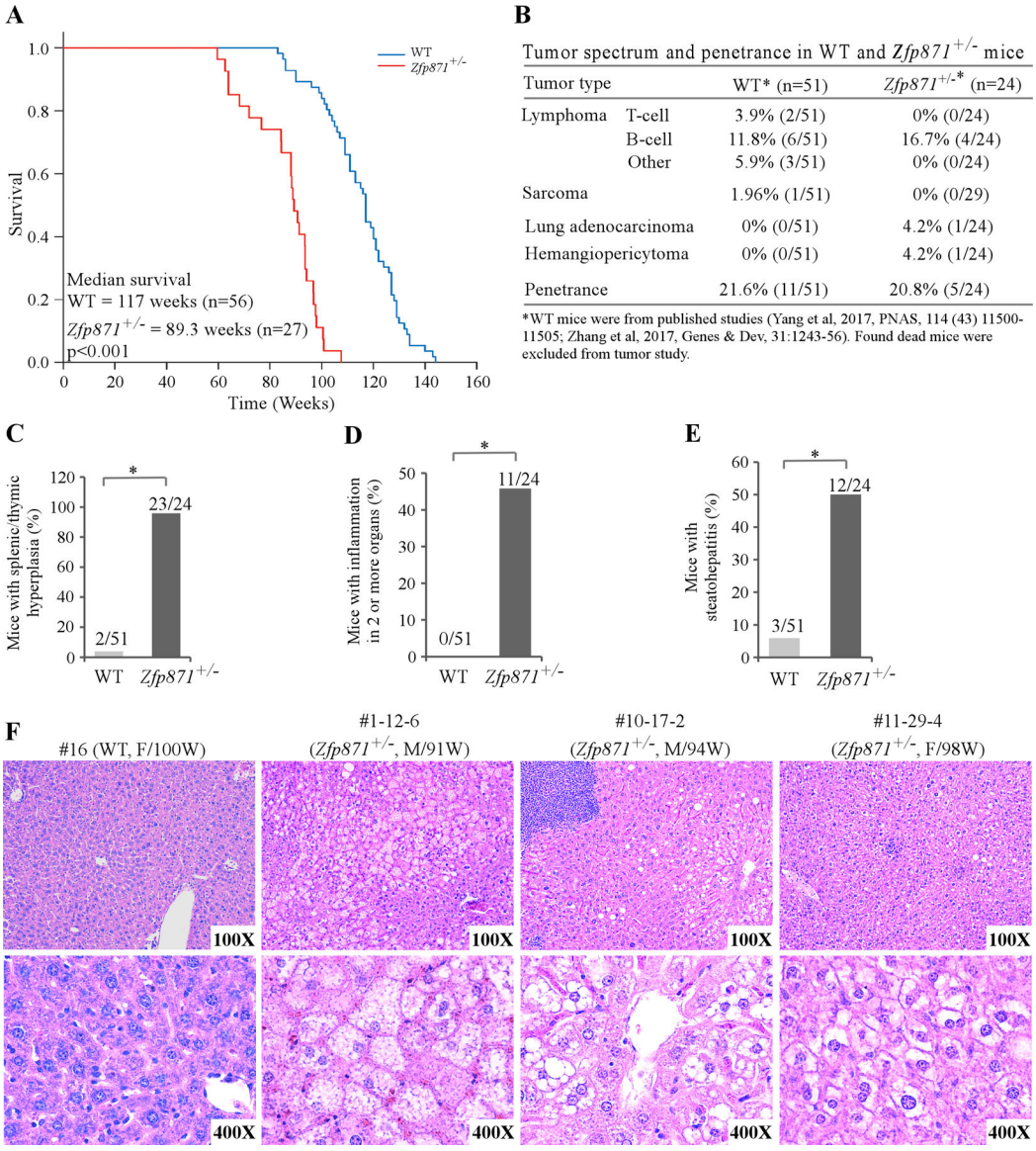

Figure 6 - *Zfp871*$^{+/-}$ mice have a short lifespan and are prone to steatohepatitis.

(**A**) Kaplan-Meier survival curve for WT and *Zfp871*$^{+/-}$ mice. (**B**) Tumor spectra and penetrance in WT and Zfp871-heterozygous mice. (**C, D, E**) The number and percentage of WT and *Zfp871*$^{+/-}$ mice with splenic and/or thymic hyperplasia (C), with inflammation in two or more organs (D), or with steatohepatitis (E). (**F**) Representative images of hematoxylin and eosin (H&E)-stained livers from a WT mouse with normal liver and three *Zfp871*$^{+/-}$ mice with steatohepatitis.